Eur Biophys J (2010) 39:1001–1006
DOI 10.1007/s00249-009-0492-3

ORIGINAL PAPER

Cl^- and F^- anions regulate the architecture of protofibrils in fibrin gel

M. Missori · M. Papi · G. Maulucci · G. Arcovito · G. Boumis · A. Bellelli · G. Amiconi · M. De Spirito

Received: 14 February 2009 / Revised: 5 May 2009 / Accepted: 13 May 2009 / Published online: 11 June 2009

Abstract Ischemic heart disease is the leading cause of serious morbidity and mortality in Western society. One of the therapeutic approaches is based on the use of thrombolitic drugs that promote clot lysis. Even if the mechanisms leading to clot lysis are not completely understood, it is widely accepted that they depend on the complex biochemical reactions that occur among fibrin fibers and fibrinolitic agents, and by their ready diffusion into the fibers. Here we investigate the effects of specific anions on the architecture of protofibrils within fibrin fibers in fibrin gels prepared in a para-physiological solution. The results obtained through small-angle X-ray scattering (SAXS) demonstrate that the characteristic axial and longitudinal repeat distances among protofibrils are strongly affected by the action of Cl^- and F^- anions.

Keywords Fibrin gel · Protofibrils · SAXS · Cl^- · F^- · Anions

Proceedings of the XIX Congress of the Italian Society of Pure and Applied Biophysics (SIBPA), Rome, September 2008.

M. Missori · M. Papi · G. Maulucci · G. Arcovito · M. De Spirito (✉)
Istituto di Fisica, Università Cattolica del Sacro Cuore, Largo F. Vito 1, 00168 Rome, Italy
e-mail: m.despirito@rm.unicatt.it

M. Missori
Consiglio Nazionale delle Ricerche, Istituto dei Sistemi Complessi, Via del Fosso del Cavaliere 100, 00133 Rome, Italy

G. Boumis · A. Bellelli · G. Amiconi
Dipartimento di Biochimica, Università di Roma "La Sapienza", Piazzale A. Moro 5, 00185 Rome, Italy

Introduction

Ischemic heart disease, which results from occlusion of one of the major coronary arteries as a consequence of thrombi and atherosclerotic plaque, continues to be the leading cause of morbidity and mortality in Western society (Liem et al. 2007), while stroke is the second leading cause of death worldwide (Stoll et al. 2008). Nowadays, in addition to prevention (Qureshi et al. 2000), it is possible to treat atherosclerotic plaque by means of invasive endovascular procedures (Horowitz and Purdy 2000). With the advent of thrombolytic agents that favor clot lysis, treatment of patients suffering from acute myocardial infarction (and, in general, from thromboembolic diseases) is greatly improved (Bell 2002).

Clots are composed of a three-dimensional fibrous network, known as fibrin gel; it is within the scaffold of this that platelets and other blood constituents get trapped, thus giving rise to the haemostatic plug (Doolittle 1984; Blombäck et al. 1994; Caracciolo et al. 2003).

The structure of fibrin gel (or fibrin clot) depends upon the polymerization conditions of fibrinogen, a glycoprotein present in the plasma of vertebrates made up of three different polypeptide chains that form an elongated trinodular molecule $\sim$45 nm long. The thrombin-catalyzed polymerization process is usually modelled (Doolittle 1984; Yang et al. 2000; Ferri et al. 2001; Mosesson et al. 2004 and references therein) through the occurrence of a number of distinct steps that lead to the formation of fibrin monomers, which subsequently undergo polymerization to produce oligomers called protofibrils. Lateral aggregation of protofibrils forms fibers whose diameters can reach measurements of hundreds of nanometers. The branching of fibers that takes place during the association of protofibrils creates the final fibrin network.

The presence of specific ions (e.g., Cl^-) can strongly influence the three-dimensional fibrin matrix by inhibiting the lateral aggregation of protofibrils (Caracciolo et al. 2003; Di Cera et al. 1997; Di Stasio et al. 1998; Papi et al. 2005). At low ionic strength ($\leq$150 mM) in particular, when lateral aggregation of protofibrils is more pronounced, coarse fibrin networks are formed (with fiber diameters of 100–500 nm and network pore diameters ranging from 3 to 100 μm), while fine fibrin networks (with fiber diameters of 8–100 nm and pore diameters as low as 0.1–0.5 μm) are produced at high ionic strength ($\geq$300 mM) (Ferri et al. 2002). The chief factor responsible for clot lysis rate is the intrinsic permeability of the fibrin network and of the individual fibers to proteolytic agents. The diffusional access from outside to proteases involved in fibrinolysis is not yet fully understood, and slow penetration within fibrin fibers has been demonstrated only for activated factor XIII (McKee et al. 1970). For this reason, the acquisition of further knowledge of fibrin network architecture and the packing arrangement of protofibrils would appear to be desirable.

The internal architecture of fibrin fibers has been intensively investigated but still is not completely understood. An elegant model of fibrin fibers (Yang et al. 2000; Doolittle 2004), based on crystallographic structures of fibrinogen as well as fibrin fragments, backed up by neutron diffraction experiments on fibrin fibers polymerised in powerful magnetic fields (Torbet et al. 1981), has recently been proposed. Such a representation of a highly ordered distribution of protofibrillar repeats, called a multibundle model, has been described in terms of a hypothetical unit cell of approximately 19 × 19 × 45 nm, within which each basic protofibrillar entity is separated by a distance of 8 nm and half-staggered in relation to adjacent protofibrils. Also in recent times, an energy dispersive X-ray diffraction (EDXD) study carried out on coarse fibrin gels induced by thrombin, prepared by clotting fibrinogen directly on to the surface of silicon wafers, has confirmed that protofibrils within fibrin fibers are packed together in a regular array (Caracciolo et al. 2003). The measured diffraction patterns obtained in these conditions confirm the well-known axial repeat distance of 22.5 nm and demonstrate the existence of a prominent ca. 18-nm reflection due to the fibers' lateral order.

In this paper we present the results of a small angle X-ray scattering (SAXS) study of the effect of NaCl and NaF in solution on the packing arrangement of protofibrils. Indeed, despite the fact that the presence of ions in solution strongly influences network architecture in terms of fiber diameter and clot porosity, no previous experimental investigation has been devoted to the study of the internal architecture of fibrin fibers in the presence of specific ions in solution.

Materials and methods

Sample preparation

Human α-thrombin was isolated from commercial thrombin preparations (Calbiochem-Novabiochem, San Diego, CA, USA) as previously described (De Cristofaro and Di Cera 1990). Plasminogen-free lyophilized human fibrinogen was procured from Calbiochem-Novabiochem (San Diego, CA, USA). In order to remove large aggregates, commercial fibrinogen was dissolved in 50 mmol/l Tris–HCl, pH 7.4, 50 mmol/l NaCl or NaF, and 1 mmol/l EDTA sodium salt, and subsequently purified by employing size-exclusion chromatography on a 100 × 1.5 cm glass column (Pharmacia Biotech, Milano, Italy) filled with sepharose CL-4B and eluted at 3 ml/h with the dissolving buffer. Fibrinogen concentration was determined spectrophotometrically by applying an extinction coefficient value of 1.51 ml mg^{-1} cm^{-1} at a wavelength of 280 nm. Gels were grown from fibrinogen solutions at monomer concentrations of 1 mg/ml in Tris–HCl 50 mM, EDTA-Na2 1 mM, and a pH 7.4 buffer with 50 mM of NaCl or NaF, according to the protocol already described (Ferri et al. 2001; Papi et al. 2005), in Eppendorf cuvettes. Next, immediately prior to SAXS measurements being taken, the gels were transferred to measurement cells (diameter 10 mm, optical path 1 mm) and sealed using 25-μm-gauge mica windows. The fibrinogen monomers were activated with thrombin at a constant molar ratio of thrombin/fibrinogen = 0.01.

SAXS

SAXS (Kerker 1969; Roe 2000) measurements were carried out using the ID02 high brilliance beamline at the European Synchrotron Radiation Facility (ESRF) at Grenoble.[1] Incident X-ray energy was fixed at 12.46 keV, and the X-ray spot on the samples was set to 300 × 300 μm. To allow for accurate subtraction of the scattering deriving from cell and solvent, solvent scattering was measured. The two-dimensional SAXS pattern was azimuthally averaged so as to obtain the scattered intensity $I(q)$ as a function of the X-ray-exchanged momentum q at a resolution of 0.003 nm^{-1}. Data were converted to absolute intensity values by normalizing to the scattering signal of water. Measurements were performed at room temperature. Each acquisition was averaged over 1 s to avoid sample damage and successively repeated at different positions on each sample to augment the number of statistics for analysis.

[1] http://www.esrf.fr/UsersAndScience/Experiments/SCMat-ter/ID02/BeamlineDescription

Results

Figure 1a shows SAXS scattering profiles, arbitrarily shifted for clarity, arising from different spots along the scattering cell, of three independent samples of fibrin gels grown in a 50 mM NaCl fully hydrated environment. Independently of both the spot and the sample chosen, the scattered intensity shows a shaped decay as the wave vector q increases. With continuous decay, minute additional contributions, localized in the q-range $0.2 < q < 0.5$ nm^{-1}, emerge. The effect of several ions on the macroscopic structure of the fibrin network is known (Di Stasio et al. 1998; Papi et al. 2005; Ferri et al. 2002). Since Cl^- and F^- are two of those anions known to induce different structural modifications at a large scale, we also investigated the SAXS scattering profile from a fully hydrated fibrin gel grown in a 50 mM NaF hydrated environment (Fig. 1b). A shaped decay, similar to that observed in gels grown in NaCl solutions and still independent of both the spot and the sample chosen, is observed. To highlight modifications, possibly occurring at nanoscopic scales, we report in Fig. 2 the SAXS scattering profile averaged across all gels left growing in buffer solution with chloride (lower curve) and with fluoride anions (upper curve) in the q range $0.15 < q < 0.6$ nm^{-1}.

Fibrin gel, grown in low concentration NaCl solutions, is know to produce an intricate network of interconnected fibers of hundreds of nanometers in diameter with a mesh size of microns (coarse fibrin gel) (Papi et al. 2005; De Spirito et al. 2003). Within the length scales probed in our experiments (roughly ranging from 10 to 100 nm), the X-ray profile is dominated by the superposition of two different contributions: the scattering from protofibrils, constituting the fibrin fibers, and Bragg diffractions due to the ordered structures inside each protofibril, proposed by R. F. Doolittle (Yang et al. 2000). To isolate the minute

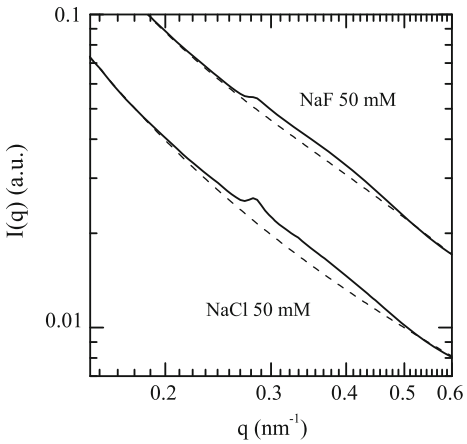

Fig. 2 Log-log plot of the averaged SAXS signals resulting from fully hydrated fibrin gel samples in 50 mM NaCl (*lower line*) and NaF solutions (*upper line*). For each sample, an increasing SAXS signal localized around 0.2−0.5 nm^{-1} can be observed. *Dashed lines* represent the sixth-order polynomial function used in data analysis (see text)

scattering contribution observed, we modelled the scattering profile with a sixth-order polynomial function (dashed lines in Fig. 2). By subtracting this contribution to the experimental data, we can produce the curves reported in Fig. 3a, b. Two superimposed, peaked contributions describe the overall shape of the region ($0.15 \leq q \leq 0.6$ nm^{-1}). These contributions, modelled as Gaussian distributions (dashed lines in Fig. 3a), give a sharp peak at $q_1 = 0.284$ nm^{-1} with a full-width-at-half-maximum (FWHM) of 0.019 nm^{-1} and a second, broader peak at $q_2 = 0.327$ nm^{-1} with an FWHM of 0.190 nm^{-1}.

The first sharp peak can be assigned to a Bragg diffraction from a repeat distance of $d_1 = \frac{2\pi}{q_1} = 22.1$ nm (± 0.2 nm) that slightly, but significatively, differs from the well-known repeat distance close to 22.5 nm along the

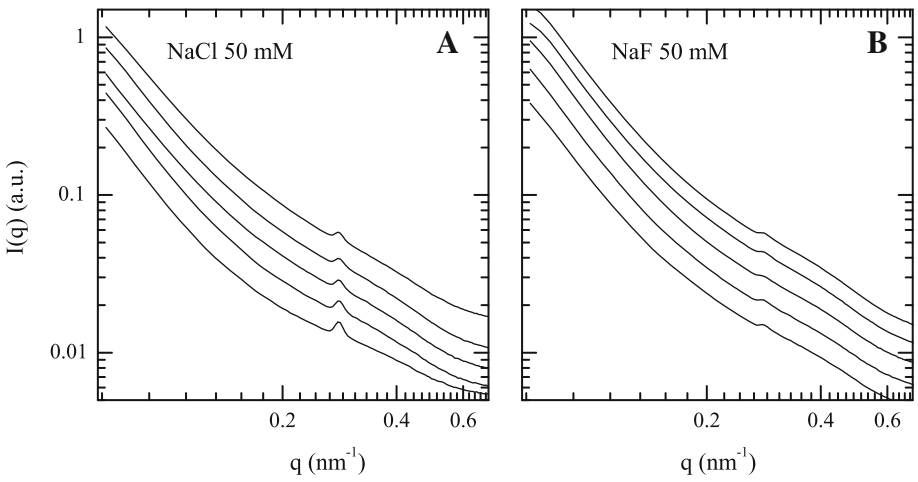

Fig. 1 Log-log plot of the SAXS signals, arbitrarily shifted for clarity, resulting from three independent samples of fully hydrated brin gel prepared in 50 mM NaCl (**a**) and in 50 mM NaF (**b**). For each sample, SAXS intensity distributions, collected from several spots along the scattering cell are also reported. Samples appear very homogeneous, as the distribution shape remains substantially unaltered

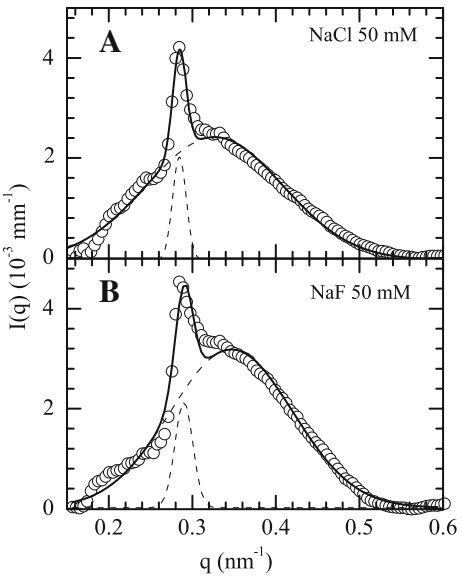

Fig. 3 SAXS signals from fully hydrated fibrin gel samples in 50 mM **a** NaCl and **b** NaF solutions, following subtraction of the smooth decreasing contribution. *Curves* have been fitted with two Gaussian functions

fiber axis (Caracciolo et al. 2003; Yang et al. 2000). The second, broader peak can instead be assigned to a Bragg diffraction from a lateral repeat distance of $d_2 = \frac{2\pi}{q_2} =$ 19.2 nm($\pm$0.2 nm).

Even in this case, a minute contribution appears localized in the region $0.2 < q < 0.5$ nm^{-1}. The minute contribution was isolated, as previously described, by subtracting, from the overall spectra, a smooth decreasing contribution given by sixth-order polynomial functions (see dashed lines in Fig. 2). The resulting curve is reported in Fig. 3b. Two scattering contributions can still be recovered: a first, sharp peak at $q'_1 = 0.290$ nm^{-1} with an FWHM of 0.025 nm^{-1} and a second, broader peak at $q'_2 = 0.347$ nm^{-1} with an FWHM of 0.172 nm^{-1}. In this case, the sharp peak corresponds to a Bragg diffraction from a repeat distance of $d'_2 = 21.7$ nm ($\pm$ 0.2 nm), while the second peak can be assigned to a Bragg diffraction from a lateral repeat distance of $d'_2 = 18.1$ nm ($\pm$ 0.2 nm).

Discussion

Under physiological conditions, chloride must be the most relevant anion affecting the fibrin clot architecture. Indeed, an exhaustive series of light-scattering experiments (Di Cera et al. 1997; Di Stasio et al. 1998; Papi et al. 2005; Papi 2005) shows that a number of ions, i.e., those that bind water weakly (e.g., perchlorate-iodide as well as chloride) associate with positively charged groups on protofibrils with significant affinity, thus inhibiting lateral aggregation (Weisel 1986). On the other hand, anions that combine tightly with water (i.e., fluoride, cacodylate) show low affinity for protein cationic sites (Collins et al. 1995). The differences between coarse and fine fibrin clots have therefore been interpreted in terms of nonspecific ionic strength effects indicating that fibrin polymerization is largely controlled by electrostatic force. Nevertheless, to our knowledge, no data are available on the role played by specific anions in controlling the protofibrils' architecture.

Table 1 Axial and lateral packing distances of the fibrin protofibrils and the corresponding FWHMs

Salt	Axial distance (nm)	FWHM (nm^{-1})	Lateral distance (nm)	FWHM (nm^{-1})
NaCl	22.1 $\pm$ 0.2	0.019	19.2 $\pm$ 0.2	0.190
NaF	21.7 $\pm$ 0.2	0.025	18.1 $\pm$ 0.2	0.172

Here we show that, by using SAXS technique, it is possible to recover structural details of fibril architecture. Evidence was found of the crystalline order of protofibrils within fibrin fibers along the longitudinal and transversal axes. The repeat distances of protofibrils within the fiber appear to be strongly influenced by the presence of Cl^- or F^- anions in solution (see Table 1). In the presence of F^- anion, which is known to exert a negligible influence in the process of fibrinogen polymerization and protofibril lateral association (Di Stasio et al. 1998), both axial and lateral repeat distances appear to be 0.4 and 1.1 nm, respectively, shorter than those reached in the presence of Cl^- anions. Interestingly, longitudinal and lateral repeat distances (Table 1) turn out to be different from those found in previous EDXD experiments (22.7–22.4 and 18.4–18.1 nm, respectively), where fibrin gels were grown in 100 mM NaCl. However powerful electrostatic interactions between fibrin molecules and silicon's positively charged surface, on which fibrin has been left to gel, could easily play a significant role that is worthy of further investigation (Caracciolo et al. 2003; Yang et al. 2000).

Furthermore, our analysis allows for more light to be shed on other hidden details of fibers. Indeed, the broadening of the observed peaks could be the result of a number of different factors (i.e., limited crystalline regions (De Spirito et al. 2008), presence of disorder within the coherent structures (Roe 2000), thermal vibration of protofibrils). Hypothesizing a finite spatial range of crystal order Δ, the FWHM allows one to measure the extent of $\Delta = \frac{2\pi}{\text{FWHM}}$ (Bale et al. 1982). In our experiments the FWHM of the axial repeat distances, 0.019 and 0.025 nm^{-1} for NaCl and NaF, respectively, indicated that the average number of ordered fibrin monomers within this distance can be

estimated as $\frac{329\text{ nm}}{22.1\text{ nm}} \cong 15$ and $\frac{245\text{ nm}}{21.7\text{ nm}} \cong 12$ for NaCl and NaF solutions, respectively, a result that compares well with 15, a value estimated on the basis of biochemical considerations (Bale et al. 1982). Similar considerations for the broader peaks at 19.2 and 18.1 nm for NaCl and NaF, respectively, yield a crystal order in a range of 33 and 37 nm, not too different from those obtained through electron-microscopy studies ($\sim$50 nm) (Weisel et al. 1987). In this case we can assume a fiber that is laterally composed of a collection of highly ordered protofibrils organized, according the multibundle model, to form approximately $\frac{33\text{ nm}}{19.2\text{ nm}} \cong 1.7$ or $\frac{37\text{ nm}}{18.1\text{ nm}} \cong 2.0$ unit cells.

In conclusion we have shown that specific anions (Cl^- and F^-) are able to modify the fibrin gel structure both at mesoscopic scales (i.e., the size of fibrin fibers and that of the mesh) and at nanoscopic scales. The small changes observed by substituting anions show that there is very little room for easy penetration within fibrin fibers of the usual fibrinolytic components, either physiologic or therapeutic, in the case of fibrin gel in para-physiological conditions. This observation is in line with structural studies (Sakharov et al. 1996) that have stressed that fibrin digestion proceeds locally through transverse cutting across fibers (where plasminogen accumulates at a concentration threefold higher than in the surrounding plasma), rather than by progressive cleavage uniformly around and/or inside the fiber. And yet, blood-clot dissolution in therapy, by applying the enzymatic approach, could be greatly advantaged in terms of the thrombolytic rate of small active proteases capable of penetrating fibrin fibers and diffusing among their meshwork.

Acknowledgements Experimental data reported in this paper were obtained at the LABCEMI (Laboratorio Centralizzato di Microscopia, Ottica ed Elettronica) of the Università Cattolica del S.Cuore di Roma (Italy) (http://webprd.rm.unicatt.it/pls/unicatt_rm/consultazione.mostra_pagina?id_pagina=20215). This research was supported by the Università Cattolica del Sacro Cuore, Rome, Italy.

References

Bale MD, Jamney PA, Ferry JD (1982) Kinetics of formation of fibrin oligomers. II. Size distributions of ligated oligomers. Biopolymers 21:2265–2277

Bell WR (2002) Present-day thrombolytic therapy: therapeutic agents-pharmacokinetics and pharmacodynamics. Rev Cardiovasc Med 3 (Suppl 2):S34–44

Blombäck B, Carlsson K, Fatah B, Hessel B, Procyk R (1994) Fibrin in human plasma: gel architectures governed by rate and nature of fibrinogen activation. Thromb Res 75: 521–38

Caracciolo G, De Spirito M, Congiu Castellano A, Pozzi D, Amiconi G, De Pascalis A, Caminiti R, Arcovito G (2003) Protofibrils within fibrin fibres are packed toghether in a regular array. Thromb Haemost 89:632–636

Collins KD (1995) Sticky ions in biological systems. Proc Natl Acad Sci 92: 5553–5557

De Cristofaro R, Di Cera E (1990) Effect of protons on the amidase activity of human α-thrombin. J Mol Biol 226:1077–1085

De Spirito M, Arcovito G, Papi M, Rocco M, Ferri F (2003) Small- and wide-angle elastic light scattering study of fibrin structure. J Appl Cryst 36:636–641

De Spirito M, Missori M, Papi M, Maulucci G, Teixeira J, Castellano C, Arcovito G (2008) Modifications in solvent clusters embedded along the fibers of a cellulose polymer network cause paper degradation. Phys Rev E 77:041801

Di Cera QD, Dang E, Ayala YM (1997) Molecular mechanism of thrombin function. Cell Mol Life Sci 53:701–730

Di Stasio E, Nagaswami C, Weisel JW, Di Cera E (1998) Cl^- regulates the structure of the fibrin clot. Biophys J 75:1973–1979

Doolittle RF (1984) Fibrinogen and fibrin. Annu Rev Biochem 53:195–236

Doolittle RF (2004) Determining the crystal structure of fibrinogen. J Thromb Haemost 2:683–689. doi:10.1111/j.1538-7933.2004.00664.x.

Ferri F, Greco M, Arcovito G, Andreasi Bassi F, De Spirito M, Paganini E, Rocco M (2001) Growth kinetics and structure of fibrin gels. Phys Rev E 63:031401

Ferri F, Greco M, Arcovito G, De Spirito M, Rocco M (2002) Structure of fibrin gels studied by elastic light scattering techniques: dependence of fractal dimension, gel crossover length, fiber diameter, and fiber density on monomer concentration. Phys Rev E 66(011913):1–13

Horowitz MB, Purdy PD (2000) The use of stents in the management of neurovascular disease: a review of historical and present status. Neurosurgery 46(6):1335–1343

Kerker M (1969) The scattering of light and other electromagnetic radiation. Academic Press, New York

Liem DA, Honda HM, Zhang J, Woo D, Ping P (2007) Past and present course of cardioprotection against ischemia reperfusion injury. J Appl Physiol 103:2129–2136

McKee PA, Mattock P, Hill RL (1970) Subunit structure of human fibrinogen, soluble fibrin, and cross-linked insoluble fibrin. Proc Natl Acad Sci USA 66: 738–744

Mosesson MW, Hernandez I, Siebenlist KR (2004) Evidence that catalytically-inactivated thrombin forms non-covalently linked dimers that bridge between fibrin/fibrinogen fibers and enhance fibrin polymerization. Biophys Chem 110:93–100

Papi M (2005) Fibrin clot architecture: modulation by anion concentration, type of proteinase, thrombin level and hydrophobicity pattern distribution along the fibrinogen Aα-chain. PhD Thesis, University of Rome "La Sapienza", Rome

Papi M, Arcovito G, De Spirito M, Amiconi G, Bellelli A, Boumis G (2005) Simultaneous static and dynamic light scattering approach to the characterization of the different fibrin gel structures occurring by changing chloride concentration. Appl Phys Lett 86:183901

Qureshi AI, Luft AR, Sharma M, Lee RG, Hopkins LN (2000) Prevention and treatment of thromboembolic and ischemic complications associated with endovascular procedures: part I—pathophysiological and pharmacological features. Neurosurgery 46(6):13441359

Roe RJ (2000) Methods of X-ray and neutron scattering in polymer science. Oxford University Press, New York

Sakharov DV, Nagelkerke JF, Rijken DC (1996) Rearrangements of the fibrin network and spatial distribution of fibrinolytic components during plasma clot lysis. J Biol Chem 271:2133–2138

Stoll G, Kleinschnitz C, Nieswandt B (2008) Molecular mechanisms of thrombus formation in ischemic stroke: novel insights and targets for treatment. Blood 112(9):3555–3562

Torbet J, Freyssent JM, Hudry-Clergeon GH (1981) Oriented fibrin gels formed by polymerization in strong magnetic fields. Nature 289:1189–93

Weisel JW (1986) The electron microscope band pattern of human fibrin: various stain lateral order and carbohydrate localization. J Ultr Molec Struc Res 96:176–188

Weisel JW, Nagaswami C, Makowski L (1987) Twisting of fibrin fibers limits their radial growth. Proc Natl Acad Sci USA 84:8991–8995

Yang Z, Mochalkin I, Doolitle RF (2000) A model of fibrin formation based on crystal structures of fibrinogen and fibrin fragments complexed with synthetic peptides. Proc Natl Acad Sci USA 97:14156–61